Title

COMPARISON OF REACTIVE AND INELASTIC SCATTERING OF H2 + D2 USING FOUR SEMIEMPIRICAL POTENTIAL ENERGY SURFACES

Author

Brown, N.J.

Publication Date

1979-02-01

Lawrence Berkeley Laboratory
UNIVERSITY OF CALIFORNIA

ENERGY & ENVIRONMENT
DIVISION

Submitted to the Journal of Chemical Physics

COMPARISON OF REACTIVE AND INELASTIC SCATTERING OF $H_2 + D_2$ USING FOUR SEMIEMPIRICAL POTENTIAL ENERGY SURFACES

Nancy J. Brown and David M. Silver

February 1979

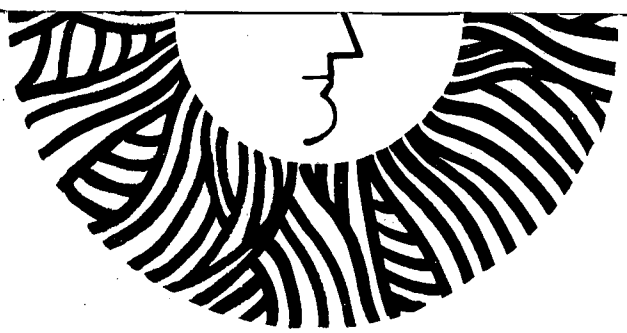

Prepared for the U.S. Department of Energy under Contract W-7405-ENG-48

DISCLAIMER

COMPARISON OF REACTIVE AND INELASTIC SCATTERING OF $H_2 + D_2$ USING FOUR SEMIEMPIRICAL POTENTIAL ENERGY SURFACES

Nancy J. Brown
Energy and Environment Division
Lawrence Berkeley Laboratory
University of California
Berkeley, California 94720

and

David M. Silver
Applied Physics Laboratory
The Johns Hopkins University
Laurel, Maryland 20810

This research was supported in part by the Office of Energy Research, Basic Energy Sciences Division of the U.S. Department of Energy under Contract No. W-7405-ENG-48 at the Lawrence Berkeley Laboratory Energy and Environment Division, and in part by the Department of the Navy, Naval Sea Systems Command under Contract No. N00024-78-C-5384 at the Johns Hopkins University Applied Physics Laboratory.

ABSTRACT

Collisions between hydrogen and deuterium molecules are examined using quasiclassical dynamical trajectory calculations with the intermolecular field specified by four semiempirical potential energy surfaces. Three of the surfaces are calculated within the valence bond model with semiempirical evaluation of the integrals, and the fourth is the London type. Various degrees of agreement are observed between these four surfaces and ab initio results. The trajectory calculations are performed at high system energies to permit the possibility of reactions. In addition to nonreactive collisions, four reaction paths are found on each surface with the product species $2H + D_2$, $H_2 + 2D$, $HD + H + D$, and $2HD$. The results are analyzed to determine the effect of surface properties on reaction probabilities, average final state properties of the molecules and average final state energy distributions. Dynamical results are found to be strongly dependent on surface characteristics.

I. INTRODUCTION

A prototype for bimolecular collision processes is the $H_2 + D_2$ system which, at suitable values of energy, is capable of undergoing elastic, inelastic and reactive collisions. Although there has been considerable effort directed toward understanding the low energy collision dynamics of the H_4 system,[1-6] considerably less attention has been devoted to the investigation of the reactive characteristics of this surface.[7-10] Our own previous work[9,10] has been concerned with the investigation of reactivity and energy transfer in two different energy regimes, each with a different potential energy surface, using quasiclassical dynamics. The first study[9] was undertaken to investigate energy transfer characteristics and reactivity via double exchange: $H_2 + D_2 \rightarrow 2HD$, at a total system energy of 159 m hartree. The potential energy surface utilized for this study was a London type (LEPS) surface which includes two-atom effects and neglects overlap integrals. This London surface has an anomalously low barrier to double exchange since it lies below the 174m hartree dissociation energy of H_2. The second study[10] used a surface constructed in the valence bond model with a semi-empirical evaluation of all integrals, including many-atom contributions. This model potential energy surface had strong repulsive characteristics and, in agreement with ab initio resuts,[11-18] had energy barriers to chemical exchange which were greater than the energy required to dissociate a single hydrogen molecule. The total system energy employed in this study was 240 m hartree which permitted the possibility of chemical exchange on this surface.

In the present work quasiclassical trajectory calculations for collisions between H_2 and D_2 are presented using four potential energy surfaces: one of the London type and three constructed within the valence

bond model. Relationships between dynamical effects and surface properties are examined.

It is known that dynamical effects are quite dependent on gross qualitative features of the potential energy surface (e.g. presence or absence of a well); however, the extent of the dependence on minor quantitative surface characteristics (e.g. depth of a well) is not well understood and may vary from system to system. Several previous studies concerned with the relationship between dynamics and surface properties have examined rotational and vibrational inelastic collisions. Alexander and Berard[19] investigated the sensitivity of vibrationally inelastic processes to the fit of an ab initio surface for the He + H_2 system. Using a fixed-angle collision model, they found both the magnitude and angular dependence of calculated vibrational transition probabilities critically dependent on the analytic surface and the criterion used to fit the ab initio points. Near resonant D_2 - D_2 vibrational energy transfer in a collinear geometry was also investigated by Alexander[1] through a quantum mechanical treatment of the dynamics on four potential energy surfaces. Near resonant V → V transition probabilities were quite sensitive to subtle variations in the potential energy surface. In a parallel study of vibrational energy transfer in the H_2 + D_2 system, Alexander[1] also found vibrational transition probabilities extremely sensitive to the choice of interaction potential. Alper and Gelb[3] investigated the temperature dependence of the rotational relaxation time of molecular hydrogen in the temperature interval 300 to 1500 K using two surfaces. Calculated relaxation times were quite sensitive to details of the surface; however, results of the two calculations did not agree quantitatively with experimental values. Ramaswamy et al. studied low temperature rotational relaxation in H_2 + D_2 using

a variety of potential forms. Calculated relaxation times were quite dependent on the surface type and did not quantitatively model the results of low temperature sound absorption measurements.

The present work investigates the effect of varying the potential energy surface within a reactive energy regime for the $H_2 + D_2$ system. The total system energy employed in these trajectory calculations is maintained at 240 m hartree which is above the H_2 dissociation energy, to permit the possibility of chemical exchange. The results are presented in terms of reaction probabilities, average final state properties of the molecules, and average final state energy distributions. Since experimental observations of the $H_2 + D_2$ system have been shown to be consistent with vibrational excitation of at least one of the reactant molecules,[20-27] different arrangements of initial energy have been considered on each of the surfaces to study reactivity.

A description of the collision dynamics and a brief description of the four potential energy surfaces is given in Section II. The results of the dynamics on the various surfaces are reported in Section III for both reactive and inelastic non-reactive cases. A discussion of the results and their relationship to surface characteristics and experimental observations follows in Section IV.

II. THE MODEL AND NUMERICAL PROCEDURE

A. Trajectory Calculations

The methods of quasiclassical collision dynamics are used to study $H_2 + D_2$ collisions on four model potential energy surfaces. The conjugate coordinates and momenta, the reduced masses, the coordinate system and the boundary conditions are defined in our previous studies.[9,10] The numerical procedures, namely the use of a fourth-order Runga-Kutta algorithm to solve the equations of motion and the use of a composite generator for random number generation, have also been described previously. Atomic units are used throughout these calculations.

A set of trajectories is defined to consist of 300 trajectories, each trajectory having an initial energy configuration identical to the other trajectories in the same set, but different values of Monte Carlo variables governing the initial orientation and phases of the reactants. To facilitate comparison between the various sets and to produce a degree of uniformity in the convergence of the Monte Carlo averaging process from one set to the next, the same collection of Monte Carlo variables is used for each of the various sets. Hence the random numbers used for the nth trajectory of one set are used for the nth trajectory of all other sets. A constant initial impact parameter of 0.1 bohr was selected for all the trajectories computed.

A given set of trajectories is characterized by a quadruple of numbers: the initial H_2 rotational quantum number, the initial H_2 vibrational quantum number, the initial D_2 rotational quantum number and the initial D_2 vibrational quantum number, and the notation $(j_{H_2}\ v_{H_2}\ j_{D_2}\ v_{D_2})$ is used to identify each particular set. In this study, initial rotational quantum numbers are chosen to be zero.

The total system energy for each trajectory set is .24 hartree; however, the initial distributions of energy between relative translational, rotational, and vibrational energy of the molecules are varied. This high system energy insures a reasonable level of reactivity so that statistically meaningful Monte Carlo averages can be obtained for reaction probabilities with relatively few trajectories.

B. Final Conditions

Since a trajectory can lead to a chemical reaciton, a simple distance criterion is not available as a means of terminating the trajectory. Instead, each trajectory is integrated for a time, t = 800 a.t.u., the two smallest inter-particle distances, r_m and r_n, are identified, and the potential energy of the system, V_s, is evaluated. The trajectory is terminated when

$$\text{Morse } (r_m) + \text{Morse } (r_n) + 5 \times 10^{-4} > V_s$$

since this implies that the molecules are no longer interacting. This criterion has been checked for several trajectories and found satisfactory.

Five different types of reaction are possible outcomes of a given trajectory:

$H_2 + D_2 \rightarrow H_2 + D_2$ (non-reactive--Case I)

$H_2 + D_2 \rightarrow 2H + D_2$ (H_2 dissociation--Case II)

$H_2 + D_2 \rightarrow H_2 + 2D$ (D_2 dissociation--Case II)

$H_2 + D_2 \rightarrow HD + H + D$ (single exchange--Case IV)

$H_2 + D_2 \rightarrow 2HD$ (double-exchange--Case V)

The procedure for determining which of these reactions has occurred involves the identification of the product species, and has been described previously[9,10]. After the particular reaction path is identified the characteristics of the energy transfer occurring in both reactive and non-reactive collisions are examined. The previously described procedure for each reactive path is used to determine the final rotational $\overline{E}_j$ and vibrational $\overline{E}_v$ energy for each molecule and the final relative kinetic energy $\overline{E}_k$.

Final rotational and vibrational states for each molecule are determined and designated by the rotational and vibrational quantum numbers, j' and v', respectively. A scattering angle χ and the maximum value of the potential energy along each trajectory, referred to as the barrier, β, are also determined. For a given set of trajectories, the averages of the kinetic, rotational and vibrational energies are computed and designated by $\langle\overline{E}_k\rangle$, $\langle\overline{E}_j\rangle$ and $\langle\overline{E}_v\rangle$, respectively. The average energy change is determined by subtracting the initial value of a particular type of energy from the corresponding average final value. The average barrier, $\langle\beta\rangle$, average scattering angle $\langle\chi\rangle$ and distribution of the final rotational and vibrational states are also determined for each trajectory set. The procedures for calculating the above quantities have also been described previously.[9,10]

C. The Potential Energy Surfaces

Four semi-emperical potential energy surfaces are employed in the present work: a full description of the surfaces has been given.[20] Three of these surfaces, designated A, B and C, correspond to a valence bond treatment[21,23] of the four electron, four atom system. They differ from one another in the form and parameterization of various multiple exchange integrals (for details, consult Table I of Reference 20). In general, the

parameterization produces strong repulsive character in the H_4 surfaces so as to mimic the properties of *ab initio* calculations.[11-18] The fourth surface, designated D corresponds to a London-type surface where all overlap and multiple exchange integrals are set to zero (for details, again see Table I of Reference 20). All four surfaces allow for every possible motion of the four atoms throughout space. When one atom is removed, surfaces A, B and C reduce to the H_3 surface of Porter and Karplus.[24] The diatomic asymptotic limit is described by a hydrogenic Morse potential.[25]

III. RESULTS

Reactivity and energy transfer characteristics are determined on four potential energy surfaces designated A, B, C, and D for five different distributions of initial vibrational and translational energy which sum to a total of 240 m hartree. The selection of the five trajectory sets is based largely on the results of our previous study. They are the sets which exhibited a propensity for a particular reaction path, and it is of interest to investigate how surface properties effect the general and specific reactivity and energy transfer.

A summary of results for the various trajectory sets is provided in Table I where the initial energy distribution according to the initial kinetic and vibrational energy of each molecule is given. Reaction probabilities associated with the various reaction paths are also listed in the table. Total reactivity is less than 50 percent for the sets considered with the exception of reactivity on surface D, the London type surface.

The high reactivity on surface D via path V is a consequence of the anomalously low barrier to double exchange that occurs on this surface; the barrier to double exchange is 116 m hartree (73 kcal/mole) for a square planar arrangement of the nuclei. Of the three valence-bond type semiempiricial surfaces A, B, and C, double exchange is considerably more probable on surface B. A low energy barrier for double exchange which is less than the H_2 dissociation energy has been found for surface B in the parallelogram-rhombus geometry. This low energy path for B is illustrated in Figure 1 which shows equipotential contour maps for the four surfaces corresponding to a parallelogram-rhombus arrangement of

the four atoms. The barrier to double exchange is $\approx$ 170m hartree ($\sim$107kcal/mol)on surface B. In this geometry the similarities between A and C are evident; however neither of these has the low energy path of B. Surface D exhibits behavior that is more similar to A and C than B in the parallelogram-rhombus geometry.

Contour plots are extremely useful in finding low-energy paths for reaction; however they usually are constructed only for highly symmetric geometries. Additional low energy paths for double exchange may exist for nonsymmetric geometries for which contour plots would be inconvenient to construct.

Table 1 reveals that surfaces B and C behave similarly for H_2 and D_2 dissociation. For scattering on surfaces B and C dissociation of a particular reactant molecule is favored when the initial vibrational energy is concentrated in that molecule rather than distributed nearly equally between the molecules. Collisions on surface D result in few dissocation reactions,and collisions on the valence bond type surface A result in less dissociation reactions than those on B and C.

A. Non-Reactive Trajectories

A summary of the characteristics of the non-reactive trajectories is given in Table II. There is little variation in the average barrier $\langle\beta\rangle$ when one compares trajectories on the three valence bond surfaces; however $\langle\beta\rangle$ is less for the collisions on the London surface than for those on the valence bond type surfaces. The apparent reason for this effect is that collisions on the valence bond type surfaces are more impulsive resembling hard sphere type interactions since they are steeply repulsive, but in contrast, collisions along the London surface tend to result in greater rotational energy transfer which removes the energy available to convert to potential energy thus resulting in lower $\langle\beta\rangle$.

The more repulsive nature of the three valence bond type surfaces relative to the London surface is further confirmed through examination of the average scattering angles $\langle\chi\rangle$ which are compared for the sets on the four surfaces and listed in Table II. Examination of the individual trajectories for the sets considered reveals that deviations from the average value are small. These small deviations indicate that the scattering angle is strongly influenced by the central force portion of the potential. Since the impact parameter is the same for each of the trajectories, the near constancy of the average scattering angles for the various sets, irrespective of the initial energy conditions, reflects the strong repulsive nature of the potential and the tendency for the collisions to resemble hard sphere interactions. The scattering angle for this limiting case of hard spheres is determined from the expression:

$$\chi = 2 \text{ arc cos } (b/d)$$

where b is the impact parameter and d is a hard sphere diameter. Taking b = 0.1 bohr and values for d of $\frac{1}{2}\, r_e$ to $2r_e$, the variation in scattering angle is 164° to 176°. Although this range brackets the values of $\langle\chi\rangle$ given in Table II for the three valence bond surfaces the trajectories are certainly more complicated than hard sphere collisions as evidenced by the variation in the redistribution of energy in the final states for the sets considered on these surfaces. In addition considerable variation in final state properties occurs for a given set for the three valence bond surfaces. The values of $\langle\chi\rangle$ for the London surface D range from 149 to 154° and these angles correspond to rather unphysical values of d, the hard sphere diameter.

One can examine the sets 0008, 0204, 0303 and 0500 to ascertain the effect of the initial vibrational energy distribution between the two molecules. These sets have the same total energy, nearly the same initial kinetic and total vibrational energy, but the vibrational energy is distributed differently between the molecules. There is a variation in the average kinetic energy transferred per collision $\langle\Delta\bar{E}_k\rangle$ for a given set with respect to the surfaces considered, and for most sets considered, $\langle\Delta\bar{E}_k\rangle$ is largest for surface D. Generally, more kinetic energy is lost when the initial vibrational energy is distributed between both molecules rather than localized in one.

If one examines rotational energy transfer for all sets, a large variation with respect to surface is noted. For the sets considered, rotational energy transfer is greatest on surface D and least on C. At short distances surface D is the least repulsive and surface C is the most repulsive which is consistent with the $\langle\chi\rangle$ determined for these surfaces. Rotational energy gain is likely to occur along the incoming trajectory for the surface with the least repulsive wall, and once the energy is transferred to the rotational degree of freedom, it is no longer available for conversion to potential energy. This is consistent with the low values of $\langle\chi\rangle$ and $\langle\beta\rangle$ calculated for the London surface, D. Although the numerical values of $\langle\Delta E_j\rangle$ for both molecules vary significantly with surface type, a common characteristic of rotational energy transfer on all the surfaces is that it increases for a given molecule when the molecule contains over sixty percent of the initial vibrational energy. The same trend noted for $\langle\Delta E_j\rangle$ is obvious when one examines histograms of final rotational state distributions. As one increases the initial vibrational energy in a molecule, the final rotational state distribution tends to be spread out to higher j' and the range of j' increases. This is illustrated in

Figures 2 and 3 which show the final rotational state distributions for the sets 0008 and 0500, respectively, where the effect is most exaggerated. This effect is likely to result from the intramolecular energy transfer of vibrational energy to rotational energy. The trajectory sets 0008 and 0500 also exhibit the least kinetic energy loss. Figures 2 and 3 illustrate the greater similarities among the three valence bond surfaces and the anomalous nature of the London surface with regard to rotational energy transfer.

With a few exceptions, the average vibrational energy gain is greatest for the molecule with the least initial vibrational energy. Significant variation in $\langle \Delta E_v \rangle$ occurs with respect to surface type for the sets considered. Generally, $\langle \Delta E_v \rangle$ is positive for both H_2 and D_2; however, exceptions to this are largely $\langle \Delta E_v(D_2) \rangle$ for 0008 and $\langle \Delta E_v(H_2) \rangle$ for 0500. For these two trajectory sets, the corresponding $\langle \Delta E_j \rangle$ is unusually large for the molecule which is initially highly vibrationally excited. Additionally $\langle \Delta E_k \rangle$ for these sets is somewhat smaller than usual which provides some evidence of intramolecular V → R energy transfer.

Finally, the effect of increasing the vibrational energy in <u>one</u> molecule at the expense of initial translational energy is estimated through comparison of 0300 with 0303 and 0300 with 0500. For all surfaces, as the initial vibrational energy of one of the molecules increases, the final average kinetic energy loss decreases, and $\langle \Delta E_v \rangle$ of that molecule decreases.

In summary, the results of the nonreactive trajectory calculations indicate the following trends. Energy transfer is dominated by T → V and T → R for all surfaces. Scattering on the London type surface D results in larger rotational energy transfer than on the other surfaces, and scattering on surface C results in the smallest rotational energy gains.

Surface C is the most repulsive at short distances while surface D is the least repulsive. While there are significant differences in the average final energy distributions in the nonreacting molecules on the four surfaces, some common trends are evident. There is some evidence for energy transfer between the internal modes, for example, as the initial vibrational energy of one molecule increases at the expense of the other, it acquires more rotational energy and often loses vibrational energy which indicates that V → R energy transfer is occurring.

B. Reactive Trajectories

Table III summarizes the average final state properties of the dissociation cases II and III for those sets where percent reactivity for dissociation is 10% or greater. Dissociation of one of the molecules is the favored type of reaction on the valence bond surfaces when that molecule contains all of the initial vibrational energy except for the zero point vibrational energy of the other molecule. The London surface is anomalous since its favored reaction path is always double exchange.

H_2 tends to dissociate more easily than D_2 for nearly equal amounts of initial vibrational energy. If one considers dissociation as an extreme case of vibrational energy transfer, this effect can be explained by the greater facility H_2 appears to have for T ↔ V energy transfer. The difference in reduced mass of the two molecules is responsible for the relative ease with which H_2 gains vibrational energy and dissociates. Consistent with this argument is that more (and a greater percentage of) initial kinetic energy is lost for the sets 0500 than the 0008 sets. For all surfaces, the effect of increasing the vibrational energy for one molecule at the expense of initial kinetic energy, while the other molecule remains in v = 0, produces an increased number of

dissociations of the excited molecule. More of the vibrational energy tends to be used for dissociation as the initial vibrational energy is increased at the expense of initial kinetic energy.

The scattering angles for dissociation reactions generally tend to be somewhat less than those associated with non-reactive trajectories. Trajectories on surface B, in particular for the sets 0500 and 0008, have scattering angles that are less than those determined for trajectories on the surfaces A and C and this may indicate a different mechanism obtains for dissociation on surface B.

The dissociative trajectories exhibit large kinetic energy losses which are substantially larger than those noted for non-reactive collisions. The increased loss in kinetic energy seen for trajectories on D accounts for the large rotational energy gains in the undissociated molecule. In contrast to D, the dissociative trajectories on the valence bond surfaces do not result in much rotational energy gain. The vibrational energy change associated with the dissociative trajectories on surface A is less than that observed for the other surfaces.

Table IV summarizes the average final state properties of the single exchange cases for those sets where collisions on at least one of the surfaces result in a single exchange reaction probability greater than 3%. Single exchange is least probable on the London surface since trajectories on it are more likely to react via the lower energy path of double exchange. Single exchange is more probable on the valence bond type surfaces B and C than it is on A, and occurs more often when both molecules are vibrationally excited. The $\langle\chi\rangle$ for the sets considered is between 68 and 105°, and these values are significantly different from

the values obtained for the non-reactive and dissociative reactions. Examination of the final vibrational state distributions of the product HD revealed that $v' \leq 2$.

Characteristics of the double exchange reaction, case V are summarized in Table V. Reactivity is greatest on surface D and least on C. The reaction probability associated with double exchange on the London surface seems independent of the initial energy distribution whereas reactivity on surfaces A and B is favored when D_2 is initially vibrationally excited. Reactivity on surface C is favored when both molecules are vibrationally excited; however the probability for single exchange on surface C is greater than that of double exchange. Reactivity is greatest on surfaces D and B; the $<\beta>$ values are lowest for surface D followed by surface B. Low energy paths have been found for both surfaces B and D and it is of interest to note that $<\beta>$ values observed for D are close to the dissociation energy of H_2 (174 m hartree), which is significantly above the 116 m hartree barrier to double exchange on D along the rectangle-square reaction path. The scattering angles observed for double exchange on the four surfaces are in the range 80 to 100°; however, those observed for the London surface are very close to 90° indicating that most double exchange reactions occur along low energy paths in geometries close to the rectangle-square geometry.

The average amount of kinetic energy transferred in the reactive double exchange reactions is inversely proportional to double exchange reactivity. The average rotational and vibrational energy entries in Table V represent averages over both product HD molecules. Vibrational energy transfer to the product molecules is more substantial than rotational energy transfer and is greater than it is for single exchange.

Vibrational excitation of HD is least for reaction on the London surface. Rotational and vibrational excitation of the product HD are quite similar on surfaces A and B. When double exchange occurs on surface C it is accompanied by a large vibrational excitation.

Figures 4 and 5 contain histograms of product HD rotational and vibrational state distributions, respectively, for the set 0303 where reasonable levels of reactivity are observed for single and double exchange reactions. These histograms illustrate some differences between the two exchange reactions on the four surfaces.

Figure 4 reveals that none of the rotational distributions are peaked at $j' = 0$. There is little difference in histogram shapes for single and double exchange on surfaces A and B. Double exchange on the London surface D has the highest probability of rotational excitation since $j'_{max} = 29$ is achieved and $j' > 12$ is quite probable.

Figure 5 shows that only the lowest vibrational states are populated as a result of single exchange reactions for surfaces A, B and C; however significant vibrational excitation is evident for double exchange reactions. In single exchange, kinetic and vibrational energy must be used to supply energy for bond breaking whereas in double exchange, bond breaking is followed by (or proceeds simultaneously with) bond formation. The final energetic requirements of the two paths are thus quite different. It is also of interest to compare the HD vibrational state distributions for double exchange on the various surfaces. The distribution associated with surface D is monotonically decreasing with v' and low values of v' are considerably more probable than high values. The distribution associated with surface B is similar to that of D. The distribution associated with reaction on A indicates no strong preference

for the specific states in the range $v' \leq 12$. The distribution associated with surface C is curious since it is bimodal, that is, one of the product molecules is in $v' \leq 2$ while the other is highly excited with $10 \leq v' \leq 12$.

IV. DISCUSSION

In comparing the non-reactive scattering on the four potential surfaces some trends emerge which are common to all surfaces. Generally, more kinetic energy is lost when the initial vibrational energy is distributed between both molecules instead of being concentrated in one of them. In addition, rotational energy gain increases for a molecule when that molecule initially contains over 60 percent of the initial vibrational energy, and this provides evidence for V → R energy transfer. The energy transfer for non-reactive collisions on all surfaces is dominated by T → R and T → V transfer.

Although some significant differences obtain when one examines the average energy transferred to the various degrees of freedom in non-reactive collisions on the three valence bond surfaces, the dynamics on these surfaces are more similar to one another than they are to those on the London surface. The valence bond surfaces are more repulsive at short distances than the London surface, and the manifestation of this is evident in values of $\langle\beta\rangle$, $\langle\chi\rangle$, $\langle\Delta E_j(H_2)\rangle$ and $\langle\Delta E_j(D_2)\rangle$ obtained for the various sets. Inelastic collisions on the London surface tend to result in greater amounts of rotational energy gain. It is likely that the differences in the average energy transferred to the various degrees of freedom on the valence bond surfaces would give rise to different values of macroscopic quantities, if they were to be calculated for the system. In this sense our results associated with inelastic collisions on the valence bond surfaces exhibit the sensitivity to surface properties noted by other investigators.[1,4,6]

For all the surfaces, the effect of increasing the vibrational energy for one molecule at the expense of initial kinetic energy, while the other molecule remains in v = 0, produces an increased number of dissociations of the excited molecule. Although double exchange is the favored reaction path on the London surface, irrespective of the distribution of initial energy, dissociation is the favored reaction on the valence bond surface when one molecule contains all the initial vibrational energy (except for the zero point energy of the other molecule). Moreover, on the valence bond surfaces, H_2 tends to dissociate more readily than D_2 for nearly equal amounts of initial vibrational energy.

The probability of single exchange is least on the London surface. Little correlation can be found among the single exchange reactions on the valence bond surfaces, which is indicative that single exchange reactions occur via different pathways on these surfaces.

There are similarities among the double exchange reactions that occur on the four surfaces. Vibrational energy transfer to the product HD molecules is more substantial than rotational energy transfer and is significantly greater than that associated with the single exchange case. The scattering angles observed for double exchange are in the range 80 to 100°.

The London surface is the least and surface C is the most repulsive at short distances. The London surface is the most reactive toward double exchange with the least vibrationally excited products while surface C is the least reactive toward double exchange with the most vibrationally excited products. Double exchange product energy distributions are quite similar for A and B.

Double exchange is most probable on the London surface where reaction probabilities greater than 40 percent are obtained, and the reaction probability is quite independent of the initial distribution of the energy. Double exchange reaction probabilities vary significantly for collisions on the valence bond type surfaces with double exchange reactivity greatest on B and least on C.

The three valence bond surfaces differ from one another in both the parameterization and the mathematical form of the triple exchange integrals, J_{abcd} which can be decomposed into triatomic and four center species. Much of the four center behavior at short distances is influenced by the triple exchange integrals, and correspondingly it is not unlikely that differences in these integrals could result in different characteristics for collisions on the three valence bond surfaces.

The $H_2 + D_2$ exchange reaction has been studied experimentally by several investigators[26-32] and most recently by Lifshitz and Frenlach[33] who studied the reaction behind reflected shocks in a single pulse shock tube. Lifshitz and Frenlach attempted to measure the H atom concentrations by monitoring Lyman -α absorption. The H atom concentrations resulted from impurities present in the shock tube, and the atoms so generated were, in part, responsible for the production of HD via the atomic chain mechanism: $H + D_2$ and $D + H_2$ occurring in shock heated mixtures of H_2 and D_2. Although the investigators had difficulty with the calibrations of H atom concentrations, their results indicate that the atomic chain mechanism could not account entirely for the production of HD measured with mass spectrometry. Under the assumption that the excess HD was produced via the molecular mechanism, they determined a rate coefficient for the reaction

$$H_2 + D_2 \rightleftarrows 2HD$$

with the value $k = 10^{14.1\pm0.8} \exp(-38000/RT)$ mole^{-1} cm^3 sec^{-1} where the reaction orders were assumed to be the stoichiometric coefficients for the reaction. While the authors provide convincing evidence for a considerable contribution to exchange from a mechanism other than the atomic chain mechanism, they comment that the low value of activation energy raises serious doubts about a four-center transition state.

Our own investigations of the $H_2 + D_2$ reaction have not revealed any low energy path with barriers commensurate with the 38 kcal/mole activation energy. While double exchange reactions occur with high probability on the London surface, the low energy reaction paths are likely to be an artifact of the London approximation.

A low energy pathway for a four center double exchange reaction is also found on the valence bond surface B for a parallelogram-rhombus arrangement of the nuclei. This surface is constructed using a number of semi-empirical approximations. In particular, surface B shares the exact same functional form as surface C, but the two have different values for the empirical parameters. This change in parameter values is responsible for the shift of energy seen in Figure 1 causing surface B to have a low rhombus barrier while surface C has a high rhombus barrier. Hence, these surfaces should not be used to "predict" the position of low energy barriers. The earlier calculations of Silver and Stevens[18] using an *ab initio* CI treatment of the H_4 system failed to uncover a geometry through which there exists a reaction path for exchange requiring less energy than the dissociation energy of the H_2 molecule. They were, of course, only able to examine a restricted number of geometries. Nevertheless, it is most probable that the low

energy pathway on surface B is simply an artifact of the parameterization and mathematical form chosen to represent the H_4 surface. It is important to emphasize that the low energy paths of surfaces D and B have barriers less than but close to H_2 dissociation energies and are thus not comparable to the 38 kcal/mole activation energies derived from experimental studies.

REFERENCES

1. M. H. Alexander, J. Chem. Phys. 59, 6254 (1973); ibid. 60, 4274 (1974).

2. G. Zarur and H. Rabitz, J. Chem. Phys. 60, 2057 (1974).

3. J. S. Alper and A. Gelb, Chem. Phys. 11, 93 (1975).

4. A. Gelb and J. S. Alper, Chem. Phys. Letters 31, 245 (1975).

5. S. Green, J. Chem. Phys. 62, 2271 (1975).

6. R. Ramaswamy, H. Rabitz, and S. Green, J. Chem. Phys. 66, 3021 (1977).

7. K. Marokuma, L. Pedersen, and M. Karplus, J. Am. Chem. Soc. 89, 5064 (1967).

8. B. Shizgal, J. Chem. Phys. 57, 3915 (1972).

9. N. J. Brown and D. M. Silver, J. Chem. Phys. 65, 311 (1976).

10. N. J. Brown and D. M. Silver, J. Chem. Phys. 68, 3607 (1978).

11. V. Magnasco and G. F. Musso, J. Chem. Phys. 46, 4015 (1967); 47, 1723 (1967); 48, 2834 (1968).

12. M. Rubenstein and I. Shavitt, J. Chem. Phys. 51. 2014 (1969).

13. O. Tapia, G. Bessis and S. Bratoz, C. R. Acad. Sci. Ser. B 268, 813 (1969); Int. J. Quantum Chem. Symp. 4, 289 (1971).

14. C. W. Wilson, Jr. and W. A. Goodard III, J. Chem. Phys. 51, 716 (1969); 56. 5913 (1972).

15. O. Tapia and G. Bessis, Theor. Chim. Acta 25, 130 (1972).

16. C. F. Bender and H. F. Schaefer III, J. Chem. Phys. 57, 217 (1972).

17. E. Kochanski, B. Roos, P. Siegbahn, and M. H. Wood, Theor. Chim. Acta 32, 151 (1973).

18. D. M. Silver and R. M. Stevens, J. Chem. Phys. 59, 3378 (1973).

19. M. H. Alexander and E. V. Bernard, J. Chem. Phys. 60, 3951 (1974).

20. D. M. Silver and N. J. Brown, to be published.

21. F. London, Z. Elektrochem. 35, 552 (1929).

22. H. Eyring and M. Polanyi, Z. Phys. Chem. Abt. B 12, 279 (1931).

23. S. Sato, J. Chem. Phys, 23, 592 (1955); Bull. Chem. Soc. Jpn. 28, 450 (1955).

24. R. N. Porter and M. Karplus, J. Chem. Phys. 40, 1105 (1964).

25. P. M. Morse, Phys. Rev. 34, 57 (1929).

26. S. H. Baeur and E. Ossa, J. Chem. Phys. 45, 434 (1966).

27. A. Burcat and A. Lifshitz, J. Chem. Phys. 47, 3079 (1967).

28. D. Lewis and S. H. Baeur, J. Am. Chem. Soc. 90, 5390 (1968).

29. S. H. Baeur and E. L. Resler, Jr., Science 146, 1045 (1964).

30. S. H. Baeur, D. Marshall, and T. Baer, J. Am. Chem. Soc. 87, 5514 (1965).

31. R. D. Kern and G. G. Nika, J. Phys. Chem. 75, 1615, 2541 (1971).

32. S. H. Baeur, D. M. Lederman. E. L. Resler, Jr. and E. R. Fisher, Int. J. Chem. Kinet. 5, 93 (1973).

33. A. Lifshitz and M. Frenlach, J. Chem. Phys. 67, 2803 (1977).

TABLE I General Characteristics of Reactivity[a]

Surface	Set	E_k	$E_v(H_2)$	$E_v(D_2)$	% Unreactive	%H_2 Dissociation	%D_2 Dissociation	%Single Exchange	%Double Exchange
A	0008	128	9.89	101.4	80.7	0	15.3	0.7	3.3
B					59.3	0	22.0	3.3	15.3
C					75.0	0	24.0	1.0	0
D					53.3	0	5.0	0	41.7
A	0204	133	46.7	58.4	91.7	0	0	3.7	4.7
B					80.7	0	0	5.3	13.7
C					93.0	0.3	0.3	5.3	1.0
D					57.7	1.0	0.7	1.0	39.7
A	0300	172	63.6	7.02	94.3	5.7	0	0	0
B					69.3	23.7	0	1.3	5.7
C					78.0	22.0	0	0	0
D					52.7	3.3	0	0.7	43.3
A	0303	130	63.6	46.3	90.7	0.3	0	3.7	5.3
B					80.7	1.3	0	4.3	13.7
C					86.0	5.0	0	7.0	1.7
D					55.0	1.0	0	1.0	43.0
A	0500	138	94.2	7.02	77.0	21.7	0	0	0.7
B					55.3	36.3	0	1.3	6.7
C					68.7	31.3	0	0	0
D					47.0	11.3	0	0.3	41.3

[a]Energy in m hartree

TABLE II Nonreactive Trajectories (Case I)[a]

Set	Surface	E_k^i	Number	$\langle\beta\rangle$	$\langle\chi\rangle$	$\langle\Delta E_k\rangle$	$\langle\Delta E_j(H_2)\rangle$	$\langle\Delta E_j(D_2)\rangle$	$\langle\Delta E_v(H_2)\rangle$	$\langle\Delta E_v(D_2)\rangle$
0008	A	128	242	203	165	-10.2	3.2	11.0	3.1	- 6.6
	B		178	204	166	- 6.7	5.9	9.1	10.8	-18.4
	C		225	208	170	-13.5	1.7	7.9	19.1	-14.8
	D		160	186	149	-19.4	8.7	19.6	8.2	-16.1
0204	A	133	275	202	169	-12.9	5.9	3.9	2.0	1.2
	B		242	205	169	-22.3	7.0	4.2	10.1	1.4
	C		279	203	172	-26.5	3.3	2.2	14.1	7.0
	D		173	185	152	-36.9	13.8	13.7	1.5	8.5
0300	A	172	283	212	168	-25.7	13.5	2.4	6.8	2.7
	B		208	216	169	-28.4	12.7	3.8	-3.8	15.5
	C		234	215	172	-34.1	8.8	1.1	6.1	17.9
	D		158	186	153	-46.6	13.9	12.7	5.0	15.3
0303	A	130	272	205	169	-15.7	7.2	2.7	3.2	1.1
	B		242	209	169	-20.6	8.4	3.1	4.8	3.0
	C		258	207	172	-18.3	4.6	1.7	4.3	6.3
	D		165	190	153	-35.2	15.6	13.1	-1.3	6.8
0500	A	138	231	205	166	-14.8	17.5	1.7	-6.7	2.3
	B		166	207	168	- 5.9	15.8	3.1	-26.0	13.1
	C		206	213	171	-13.1	13.2	0.8	-15.3	14.2
	D		141	185	154	-10.4	19.1	10.7	-31.0	12.0

[a]Energy in m hartree

TABLE III Dissociation (Cases II and III)[a]

Set	Surface	E_k	Number	$\langle\beta\rangle$	$\langle\chi\rangle$	$\langle\Delta E_k\rangle$	$\langle\Delta E_j(D_2)\rangle$	$\langle\Delta E_v(D_2)\rangle$
0300	A	172	17	208	169	-109.1	0.8	- 0.5
	B		71	201	156	-115.1	1.0	4.1
	C		66	195	168	-114.4	0.3	4.7
	D		10	202	148	-127.0	6.9	10.3
0500	A	138	65	201	159	- 81.1	0.4	1.3
	B		109	202	124	- 82.8	1.1	2.3
	C		94	201	159	- 83.0	0.2	3.2
	D		34	195	152	- 92.5	10.8	2.4

Set	Surface	E_k	Number	$\langle\beta\rangle$	$\langle\chi\rangle$	$\langle\Delta E_k\rangle$	$\langle\Delta E_j(H_2)\rangle$	$\langle\Delta E_v(H_2)\rangle$
0008	A	128	46	209	162	- 71.7	1.1	-0.1
	B		66	202	132	- 74.1	1.3	1.5
	C		72	195	166	- 73.2	0.5	1.7
	D		15	193	158	- 76.9	5.3	1.8

[a]Energy in m hartree

TABLE IV Single Exchange (Case IV)[a]

Set	Surface	E_k	Number	$\langle\beta\rangle$	$\langle\chi\rangle$	$\langle\Delta E_k\rangle$	$\langle E_j(HD)\rangle$	$\langle E_v(HD)\rangle$
0008	A	128	2	219	67.7	-70.5	0.6	7.4
	B		10	213	88.2	-87.7	12.6	13.3
	C		3	211	87.9	-71.2	1.8	8.1
	D		0	—	—	—	—	—
0204	A	133	11	218	87.0	-88.4	6.5	13.4
	B		16	205	85.9	-86.9	8.0	10.7
	C		16	208	91.1	-87.6	5.1	13.9
	D		3	198	91.9	-97.5	16.9	12.2
0303	A	130	11	215	92.9	-86.4	11.5	9.5
	B		13	202	104.8	-88.9	11.4	13.2
	C		21	207	92.2	-81.5	2.9	13.4
	D		3	207	81.5	-98.0	10.3	24.6

[a] Energy in m hartree

TABLE V Double Exchange (Case V)[a]

Set	Surface	E_k	Number	$\langle\beta\rangle$	$\langle\chi\rangle$	$\langle\Delta E_k\rangle$	$\langle E_j(HD)\rangle$[b]	$\langle E_v(HD)\rangle$[b]
0008	A	128	10	220	82.3	-48.4	12.3	67.7
	B		46	204	87.9	-36.0	12.7	61.3
	C		0	—	—	—	—	—
	D		125	174	90.2	-14.1	17.8	45.3
0204	A	133	14	220	90.7	-43.8	11.4	63.2
	B		41	206	86.7	-30.0	10.6	57.2
	C		3	211	91.6	-81.0	2.5	90.7
	D		119	170	90.4	-12.5	16.9	42.1
0300	A	172	0	—	—	—	—	—
	B		17	203	96.6	-51.2	9.7	51.2
	C		0	—	—	—	—	—
	D		130	174	90.8	-19.4	9.6	35.4
0303	A	130	16	218	86.6	-41.9	9.3	66.0
	B		41	206	91.0	-28.2	10.0	58.5
	C		5	216	90.6	-87.3	9.3	88.6
	D		129	173	90.2	- 8.5	14.9	43.7
0500	A	138	2	227	88.0	-26.6	15.9	47.9
	B		20	203	99.1	-27.1	13.3	50.9
	C		0	—	—	—	—	—
	D		124	177	90.5	- 2.2	9.8	42.0

[a] Energy in m hartree.

[b] Average of both product molecules.

LIST OF FIGURES

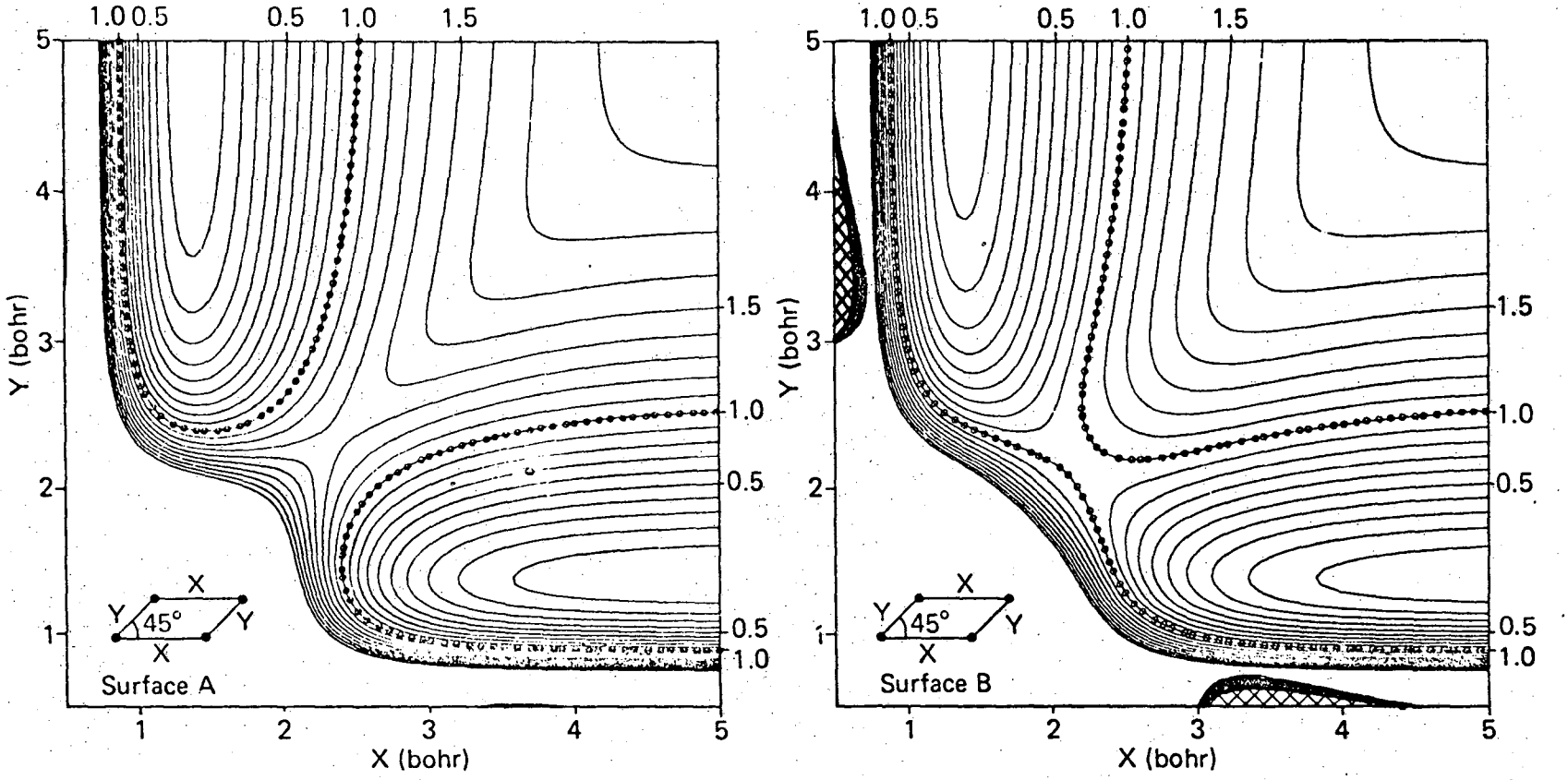

Figure 1a. Equipotential contour maps for the three semi-empirical valence bond type surfaces A through C and the London surface D, corresponding to a 45° parallelogram-rhombus arrangement of the four atoms. The contour intervals are 1/10 of the H_2 dissociation energy.

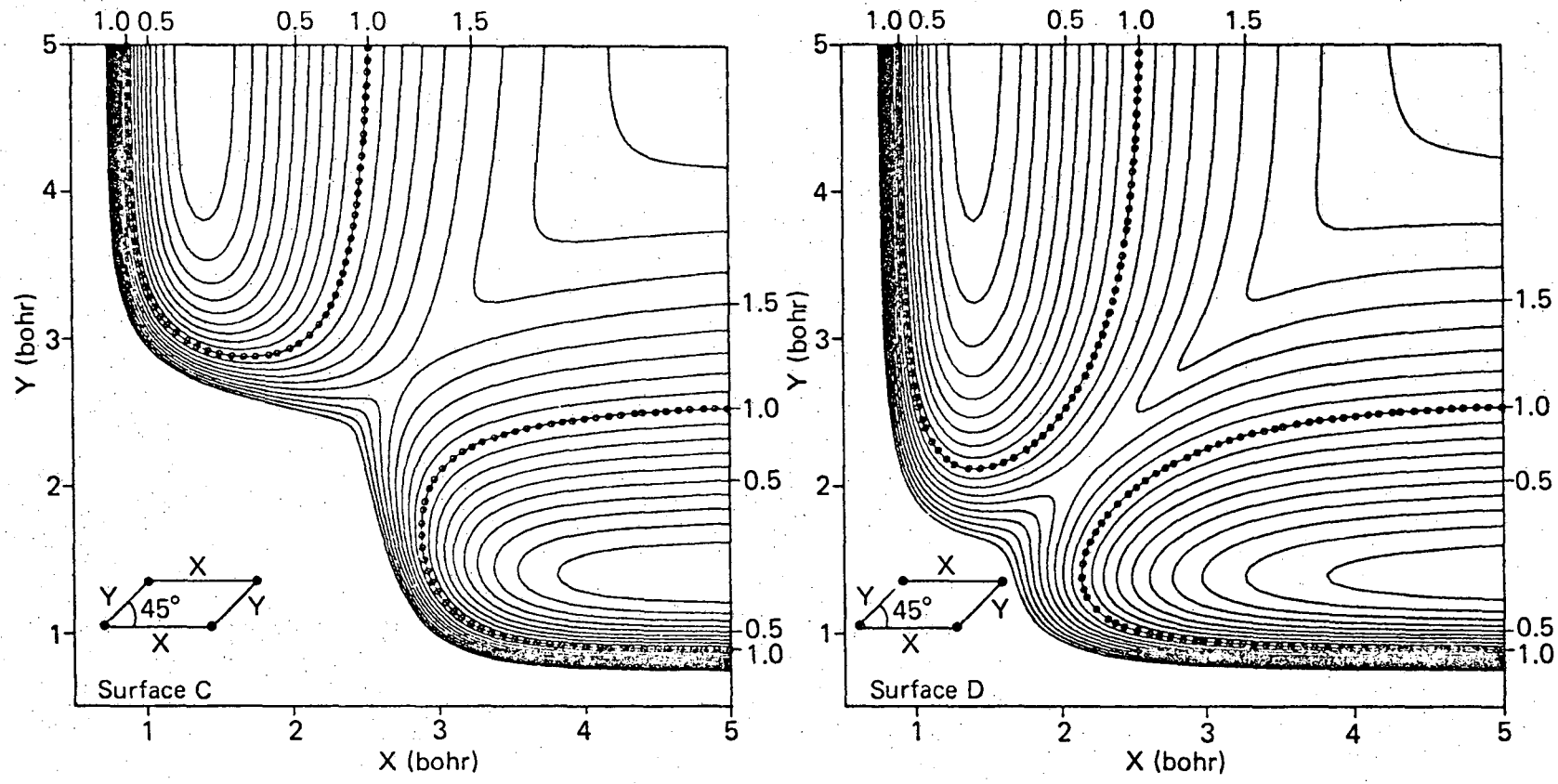

Figure 1b. Equipotential contour maps for the three semi-empirical valence bond type surfaces A through C and the London surface D, corresponding to a 45° parallelogram-rhombus arrangement of the four atoms. The contour intervals are 1/10 of the H_2 dissociation energy.

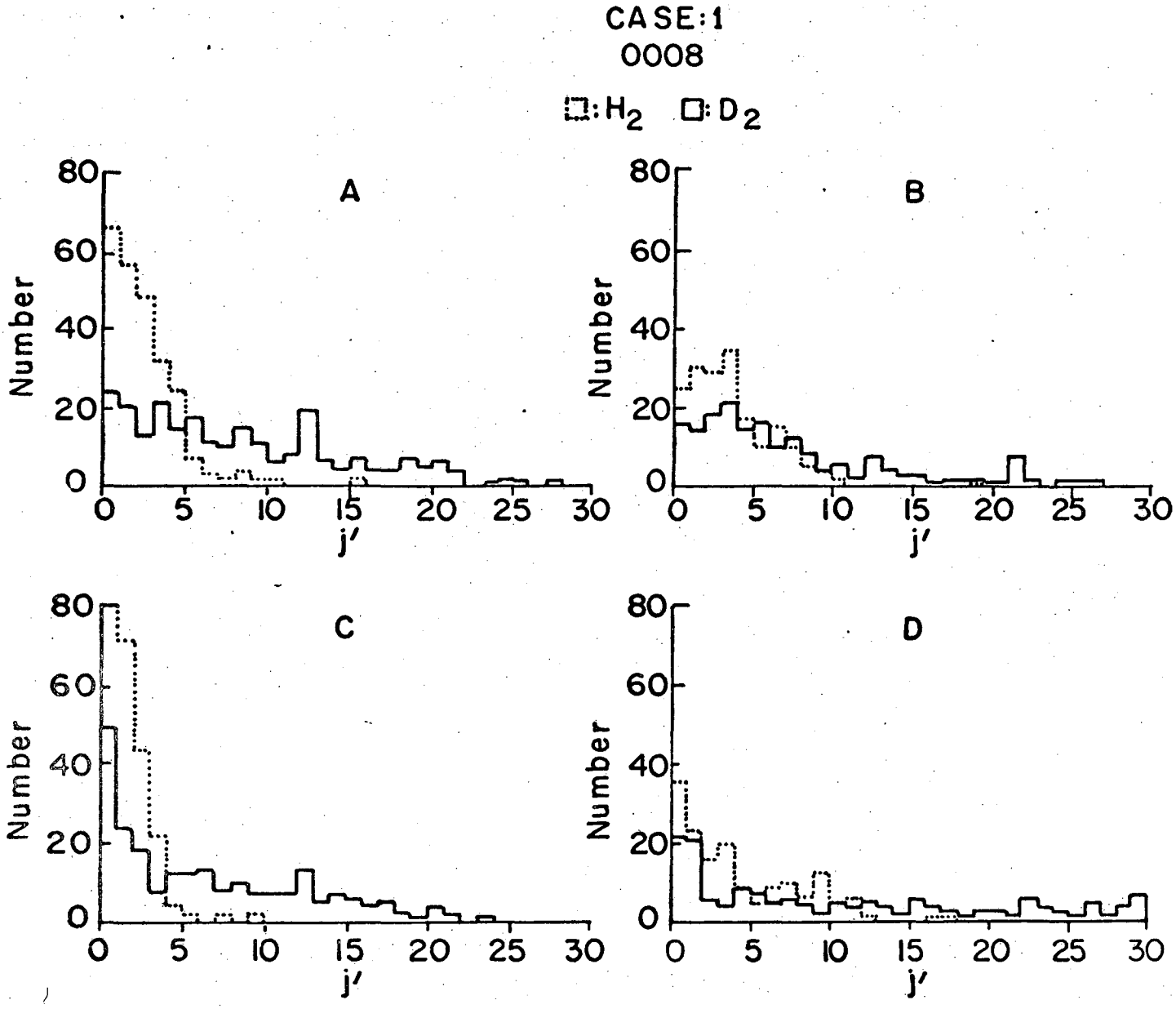

Figure 2. Distribution of final rotational (j´) states of H and D after nonreactive trajectories for the set 0008.

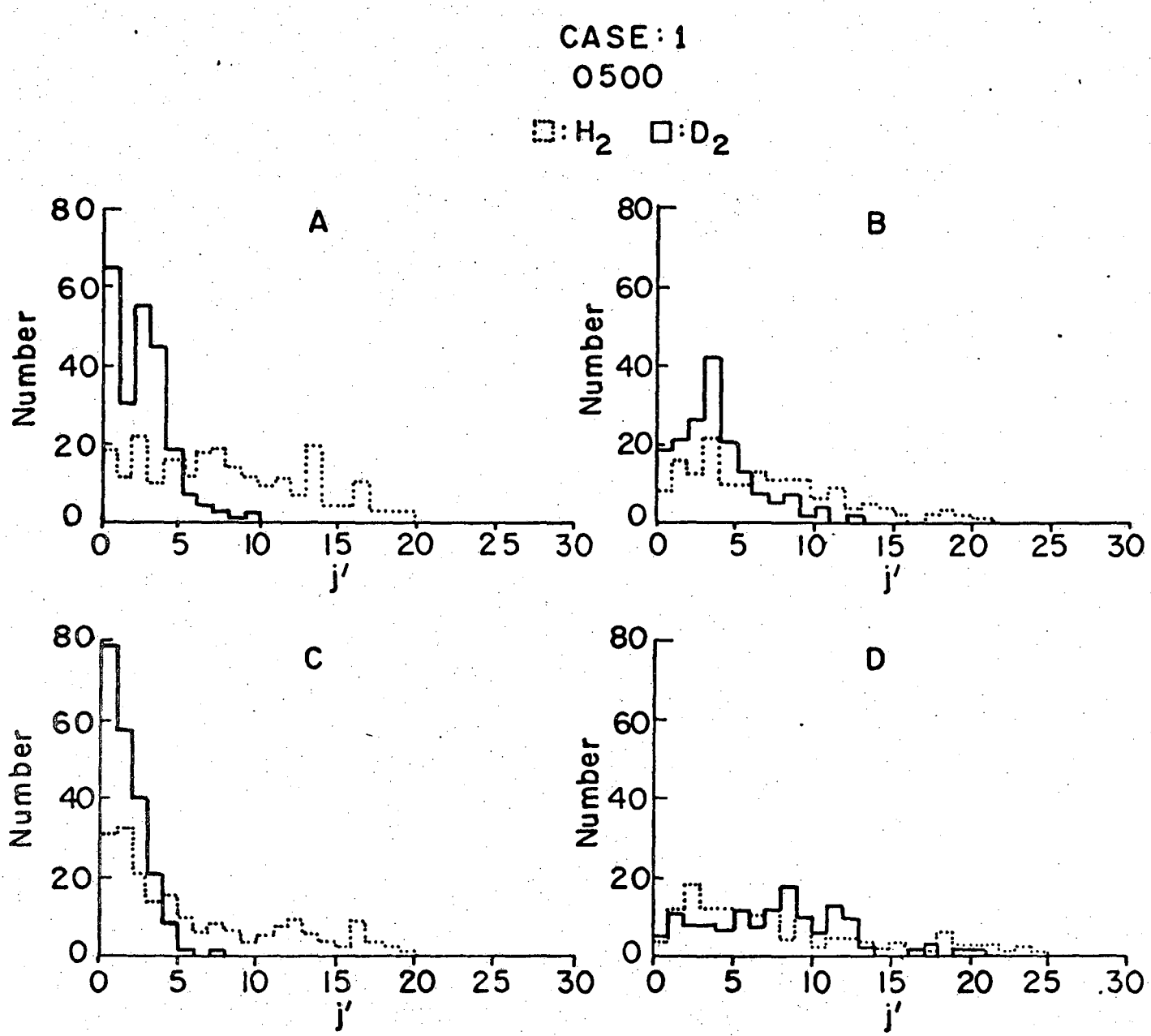

Figure 3. Distribution of final rotational (j´) states of H and D after nonreactive trajectories for the set 0500.

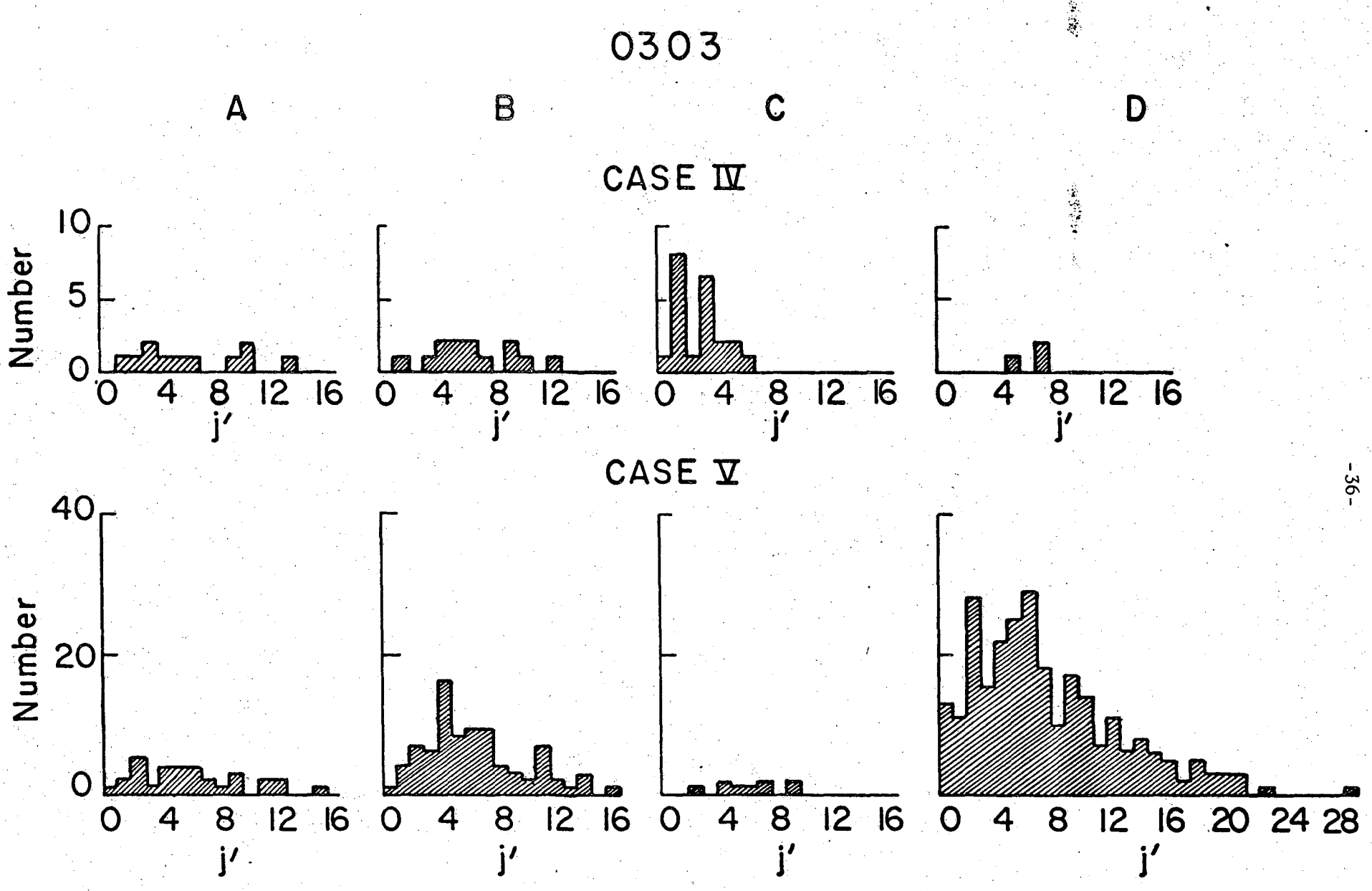

Figure 4. Distribution of final rotational (j′) states of HD after single and double exchange reactive trajectories for the set 0303.

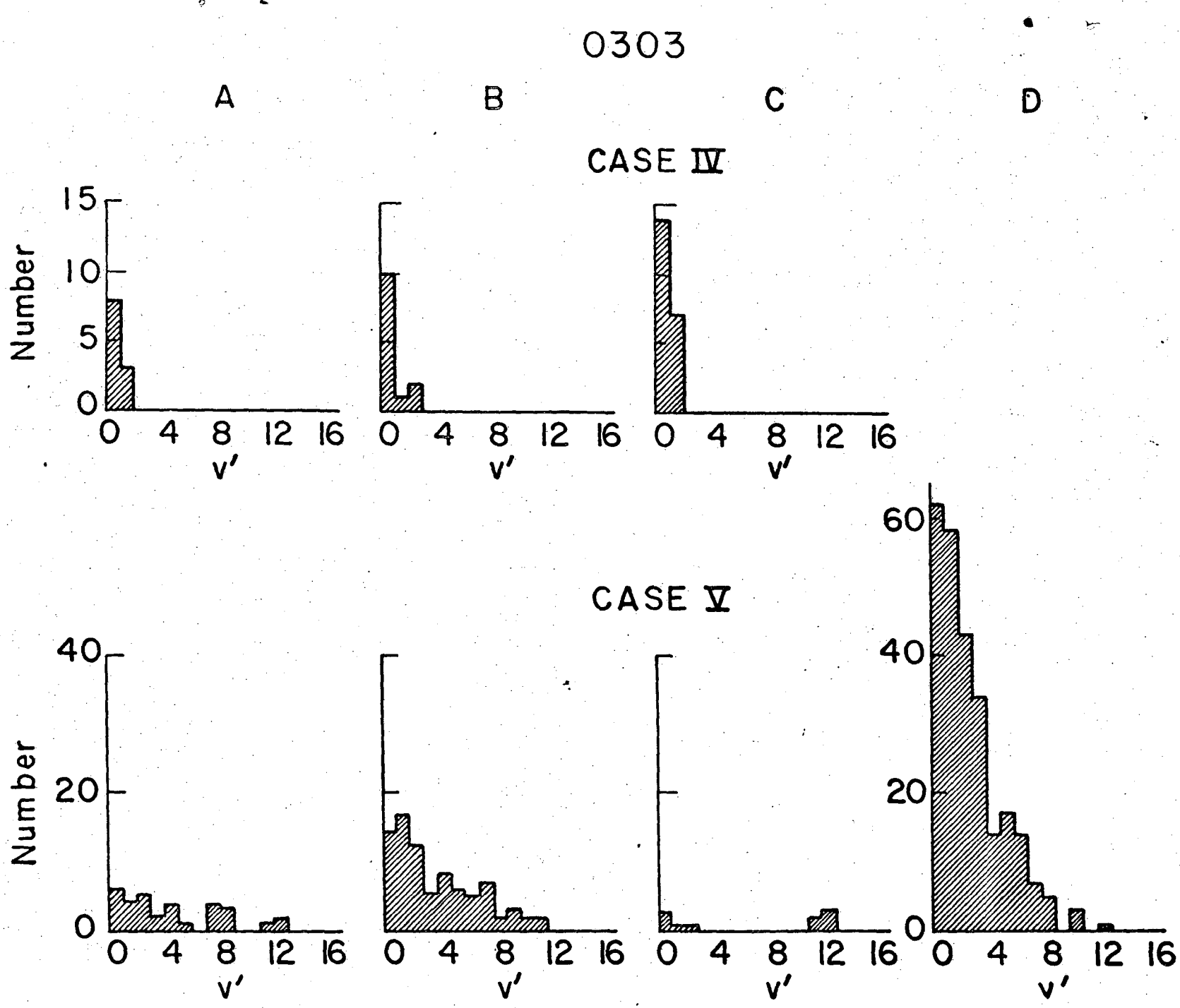

Figure 5. Distribution of final vibrational (v′) states of HD after single and double exchange reactive trajectories for the set 0303.

TECHNICAL INFORMATION DEPARTMENT
LAWRENCE BERKELEY LABORATORY
UNIVERSITY OF CALIFORNIA
BERKELEY, CALIFORNIA 94720